RESEARCH PAPER

PCCP
www.rsc.org/pccp

The $S_1Y_Z^{\bullet}$ metalloradical intermediate in photosystem II: an X- and W-band EPR study

Dionysios Koulougliotis,[abc] Christian Teutloff,[c] Yiannis Sanakis,[ad] Wolfgang Lubitz[b] and Vasili Petrouleas*[a]

[a] *Institute of Materials Science, NCSR "Demokritos", 15310 Aghia Paraskevi Attikis, Greece. E-mail: vpetr@ims.demokritos.gr; Fax: +302106519430; Tel: +302106503344*

[b] *Max-Planck-Institut for Bioinorganic Chemistry, Stiftstr. 34-36 D-45470 Mülheim an der Ruhr, Germany*

[c] *Max-Volmer-Lab., Technische Uni. Berlin, PC 14 Strasse des 17. Juni 135 10623 Berlin, Germany*

[d] *Departement of Biological Applications and Technologies, University of Ioannina, 45110 Ioannina, Greece*

Received 17th May 2004, Accepted 29th July 2004
First published as an Advance Article on the web 16th August 2004

Visible light illumination at liquid He temperatures of photosystem II (PSII) membranes poised in the S_1-state, results in the production of a metalloradical signal with resonances at $g = 2.035$ and $g \sim 2.0$ at X-band (J. H. A. Nugent, I. P. Muhiuddin, and M. C. W. Evans, *Biochemistry*, 2002, **41**, 4117–4126). A similar signal has been obtained by near IR excitation of samples poised in the S_2 state (D. Koulougliotis, J.-R. Shen, N. Ioannidis, and V. Petrouleas, *Biochemistry*, 2003, **42**, 3045–3053). The signal has been attributed to the magnetic interaction of the tyrosyl Z radical with the Mn cluster in the S_1 state. In an effort to obtain further information about the interactions of tyrosine Z with the Mn cluster, and about the integer-spin S_1 state we have employed EPR spectroscopy at two frequencies, X and W-band. The spectrum at W band is characterized by novel resonances at $g = 2.019$, $g \sim 2.00$ and $g = 1.987$. For the analysis of the spectra at the two microwave frequency bands a spin Hamiltonian has been applied under the following basic assumptions: The S_1 state of the Mn cluster is characterized by two low lying spin states $S_a = 0$ and 1. The major features of the spectra are attributed to the interaction of the $S_a = 1$ state with the spin $S_b = 1/2$ of the tyrosyl radical. Potential contributions from the $S_a = 0$ state are suppressed under the present experimental conditions. A satisfactory fit reproducing all features of the spectra is achieved with the same set of fitting parameters for the signals at both bands. An anisotropic ferromagnetic exchange interaction results from the fit with the coupling value being of the same order of magnitude with the value of the zero field splitting term of the Mn cluster ($S = 1$).

Introduction

Photosystem II (PSII) is a multisubunit membrane–protein complex that catalyzes the light-driven oxidation of water to dioxygen in green plants, algae and cyanobacteria. The three-dimensional structure of PSII has been recently made available at 3.5–3.8 Å resolution by X-ray crystallography.[1–3] It reveals the subunit molecular architecture as well as the spatial organization of the redox cofactors involved in the electron transfer chain. The location of two unique tyrosine residues found in PSII known as Tyr Z (Tyr 161 of the D1-polypeptide) and Tyr D (Tyr 160 of the D2-polypeptide) is also revealed in the electron density maps.

Tyr D is present in the form of a stable radical ($Y_D^{\bullet}$) displaying a characteristic X-band EPR spectrum known as signal II. Its physiological role is not precisely known[4] and it is not involved in the normal electron transfer reaction chain. Tyr Z is in close proximity to the tetranuclear Mn-cluster (known also as the O_2-evolving complex, OEC) as indicated by EPR studies[5–9] and depicted in the X-ray crystallographic data. Models suggesting a direct involvement of Tyr Z in the water oxidation process have been proposed.[10–16] During the water oxidation process, the OEC cycles between five oxidation states (S_0–S_4), the numerical subscript denoting the number of accumulated oxidizing equivalents in each state. Cycling through the S-states is activated by sequential photon absorption by PSII. Oxygen evolves during the S_3 to S_0 transition (S_4 being a transient state). The dark stable oxidation state is S_1.[17]

Significant interest has been shown in the trapping and study of Tyr Z. In PSII preparations lacking the Mn cluster Tyr Z can be trapped in the $Y_Z^{\bullet}$ neutral radical form. Under these conditions $Y_Z^{\bullet}$ gives rise to a free radical EPR signal at X-band similar to that of $Y_D^{\bullet}$. In PSII preparations in which advancement to the S_3-state is inhibited by different treatments as for example addition of acetate or calcium depletion a broad EPR signal (100G–230G wide) is observed. This signal was assigned to the $Y_Z^{\bullet}$ radical interacting with the S_2-state of the OEC. Theoretical simulations of this EPR signal implied spatial proximity of Y_Z and the OEC.[5–9]

During the last years high-frequency high-field (HF) EPR spectroscopy has been applied to study structural and functional aspects of PSII. HF EPR provides important complementary information to the conventional X-band EPR at 9 GHz. For example, the large magnetic fields utilized in HF-EPR can resolve the *g*-tensor components of the observed radicals, provide novel information on the nature of the g-anisotropy, distinguish between overlapping radicals, elucidate the nature of their local chemical environment etc.

Both $Y_D^{\bullet}$ and $Y_Z^{\bullet}$ have been studied by HF-EPR spectroscopy at different frequencies in the presence or absence of the OEC. From these studies the *g*-tensor values for these radicals have been determined.[20] In Mn-containing intact PSII

DOI: 10.1039/b407355j

preparations (single crystals of PSII of core complexes from the thermophilic cyanobacterium *Thermosynechococcus elongatus*), HF-EPR measurements were applied for the determination of the magnitude and orientation of the *g*-tensor of $Y_D^{\bullet}$.[21]

A detailed HF-EPR study of the $Y_Z^{\bullet}$ radical in Mn-containing PSII preparations (with the OEC poised in the S_2-oxidation state) was recently carried out at three different frequency bands: 95, 190 and 285 GHz.[9] The OEC in these preparations was inhibited by addition of acetate or by depletion of the calcium cofactor. The magnetic interaction of $Y_Z^{\bullet}$ with the S_2-state of the OEC gives rise to a metalloradical type EPR signal denoted $S_2Y_Z^{\bullet}$. The experimental EPR spectra obtained at all four EPR frequencies (9, 95, 190, 285 GHz) were fit simultaneously in order to explore the nature of the coupling between the radical and the manganese cluster. The sign of the exchange spin–spin coupling was determined and it was shown to depend on the sample treatment: antiferromagnetic in calcium-depleted preparations and ferromagnetic in acetate-treated preparations. This study showed the usefulness and need of variable-frequency EPR spectroscopy in characterizing the magnetic interaction between two spin systems.

Recently a metalloradical type signal at X-band attributed to $S_1Y_Z^{\bullet}$ was observed in intact PSII preparations. This signal is induced by two different illumination protocols at cryogenic temperatures (<20 K): either visible light illumination of O_2-evolving PSII membranes poised in the S_1-state[22] or near-infrared illumination of samples poised in the S_2-state.[23] In the former case illumination leads to charge separation and the oxidation of Tyrosine Z by P_{680}^{+} (the advancement of the Mn cluster from the S_1 to the S_2 state is inhibited at liquid helium temperatures). In the latter case the Mn cluster excited by the NIR illumination is believed to act as the oxidant of Tyrosine Z.

In the present work, EPR studies at X- and W-band frequencies together with a theoretical analysis of the experimental spectra are employed in order to characterize this $S_1Y_Z^{\bullet}$ metalloradical intermediate and explore the nature of the magnetic interaction between the two spin systems ($Y_Z^{\bullet}$ and the Mn cluster in the S_1 state).

Materials and methods

PSII-enriched membranes from market spinach (BBY preparations) were isolated by standard procedures[24,25] with some modifications. Samples for EPR measurements were suspended in a pH 6.5 buffer containing 0.4 M sucrose, 15 mM NaCl and 40 mM MES, at a final chlorophyll concentration of 6–8 mg Chl ml^{-1}, and subsequently stored in liquid nitrogen (N_2). In order to enhance the $S_1Y_Z^{\bullet}$ signal,[22,23] the BBY membranes were supplemented with exogenous quinones, typically 1 mM DCBQ (2,5-dichlorobenzoquinone), from a stock solution in DMSO.

Samples were poised in the S_1-state by dark adaptation at 273 K for 1 h. In the X-band EPR measurements, continuous visible light illumination of BBY membranes was performed in the EPR cavity at liquid He temperatures (typically between 10 K and 12 K) for a time period of 3–5 min. A 340 W projector lamp filtered with a combination of a 3 mm BG39 filter (absorbing above 650–750 nm) and a saturated $CuSO_4$ solution, in order to select visible light, was employed. Samples were allowed to equilibrate for 2 min after the illumination period before spectra were obtained. In the W-band EPR measurements, light excitation of the samples was achieved with a Q-switched, frequency-doubled Nd:YAG laser from Quanta Ray (DCR with SHG-2) operating at a repetition rate of 10 Hz. The laser beam was coupled into an optical fiber which was directly aligned on top of the sample. The EPR spectrum was collected with the laser light on and lasted approximately 20 min at a temperature approximately equal to 10 K. The light-induced EPR signal attributed to the $S_1Y_Z^{\bullet}$ metalloradical intermediate decayed fast even at liquid He temperatures (complete decay in 20–30 minutes at 11 K) *via* recombination with the reduced quinone acceptor, Q_A^{-}.[22,23] Visible-light illumination at 11 K, induced also a small amount of carotenoid radical ($Car^{\bullet+}$) in the $g = 2.0$ region of the EPR spectrum, which however decays in a much slower timescale at liquid He temperatures.[26] Thus, EPR spectra of the $S_1Y_Z^{\bullet}$ metalloradical intermediate are obtained by taking the difference of the light-induced spectrum minus the one obtained after remaining in the dark at 11 K for at least 20 min.

X-band EPR measurements were performed with a Bruker ER-200D-SRC spectrometer interfaced to a personal computer and equipped with an Oxford ESR 900 cryostat, an Anritsu MF76A microwave frequency counter, and a Bruker 035M NMR gaussmeter. The temperature was calibrated with a thermocouple placed inside a test sample. Typically the spectra obtained are an average of two scans, by using 4 mm standard EPR tubes. EPR measurements at W-band were performed using a Bruker Elexsys E680 spectrometer equipped with an Oxford CF935 helium cryostat. The magnetic field was calibrated against a Li:LiF sample ($g = 2.002293$)[27] at two different frequencies. The sample tubes were quartz tubes with an outer diameter of 0.87 mm. The spectra reported are averages over 16 scans.

Theoretical simulations of the EPR spectra were performed by using a simulation program kindly provided by Prof. M. Hendrich (Dept of Chemistry, Carnegie Mellon University).[28] This program allows for simultaneous fitting of the spectra recorded at different frequencies. The spectral analysis was done in the context of the following spin-Hamiltonian:

$$H = \beta \boldsymbol{B}\cdot\boldsymbol{g}_a\cdot\boldsymbol{S}_a + \beta \boldsymbol{B}\cdot\boldsymbol{g}_b\cdot\boldsymbol{S}_b + D(S_{az}^2 - 2/3) + E(S_{ax}^2 - S_{ay}^2) + \boldsymbol{S}_a\cdot\boldsymbol{J}\cdot\boldsymbol{S}_b \quad (1)$$

In the above Hamiltonian, the basic assumption is that the EPR signals are due to the magnetic interaction of two spin systems: Spin a corresponds to the tetranuclear Mn-cluster poised in the S_1-oxidation state, and spin b corresponds to the organic radical attributed to tyrosine Z ($Y_Z^{\bullet}$) with $S_b = 1/2$. The first two terms of eqn. (1) are the Zeeman terms for the two interacting spins. The third and fourth terms correspond to the zero-field splitting terms (axial and rhombic respectively) of spin a (*i.e.* of the Mn-cluster in the S_1-state). Finally, the fifth term of eqn. (1) corresponds to the exchange coupling between the two spins a and b. No dipolar or hyperfine terms were included in the Hamiltonian (but see Results and Discussion).

The EPR simulation program performs spectral calculations by full diagonalization of eqn. (1) and polycrystalline summation. The line width is modeled with a homogeneous spin-packet linewidth; a Gaussian distribution in the values of *D*, *J* and the g_z and g_x values of spins a and b respectively was employed for achieving satisfactory reproduction of the lineshapes in both X and W-band EPR spectra. The details of the parameters employed and obtained by the simulations will be presented in the Results and Discussion section.

Results and discussion

The $S_1Y_Z^{\bullet}$ metalloradical EPR signal at X-band

To produce the $S_1Y_Z^{\bullet}$ signal, samples in the S_1 state were illuminated with visible light at 11 K (see Materials and Methods). Fig. 1 displays the difference between the spectra recorded 2 and 20 min after the end of the illumination period. The 20 min interval is sufficient for the decay of the $S_1Y_Z^{\bullet}$ signal.

The spectrum consists of a feature at $g = 2.035$ and a derivative shaped component at $g \sim 2.00$. The $g = 2.035$ feature is easily discernible even in the raw illuminated spectrum prior to the subtraction. The $g \sim 2.00$ component falls in the region where other light sensitive signals can potentially

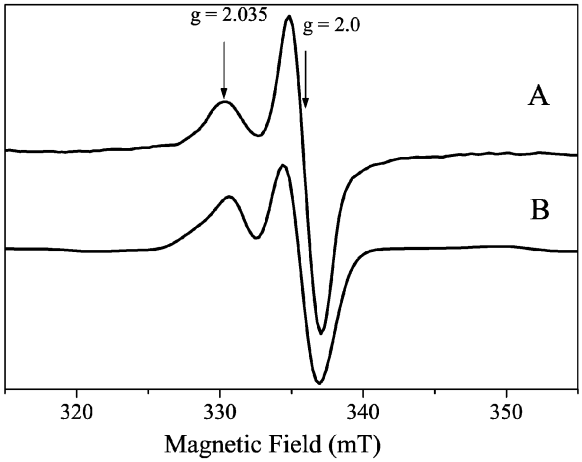

Fig. 1 A. The $S_1Y_Z^{\bullet}$ signal obtained as a difference between the spectra recorded 2 and 20 min after the end of a 5 min visible-light-illumination period of BBY membranes initially poised in the S_1 state. B. Theoretical simulation by employing spin-Hamiltonian (1) (see text for details on the simulation parameters). EPR conditions: temperature 11 K, microwave frequency 9.42 GHz, microwave power 31.7 mW, modulation amplitude 1 mT. The spectra used for the subtraction were an average of 2 scans.

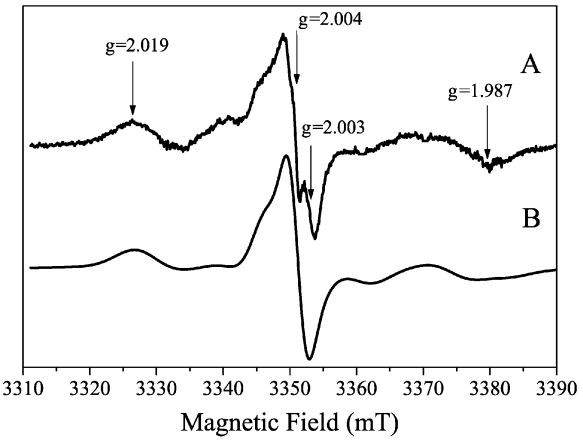

Fig. 2 A. The $S_1Y_Z^{\bullet}$ signal at W band obtained as a difference between the spectrum recorded during visible light illumination minus the spectrum obtained approximately 1 hour after the end of the 20 min illumination period in samples initially poised in the S_1-state. B. Theoretical simulation by employing spin-Hamiltonian, eqn. (1) (see text for details on the simulation parameters). EPR conditions: temperature 10 K, microwave frequency 94 GHz, microwave power 0.16 mW, modulation amplitude 1 mT. The absolute spectra (illuminated and dark adapted after the end of the illumination period) used for the subtraction were an average of 16 scans.

contribute. As noted in the Materials and Methods section the $g \sim 2.00$ component contains none (or very little) contamination from the $Car^{\bullet+}$ radical, because the latter does not decay as fast as $S_1Y_Z^{\bullet}$ during the 20 min dark incubation period at liquid He temperatures. Detailed power saturation studies, as well as experiments conducted in samples washed with NO or treated with ascorbate (in order to reduce the $Y_D^{\bullet}$ background EPR signal) show that a large part of the light induced signal at $g \sim 2.00$ is distinct from $Y_D^{\bullet}$. These experiments will be presented in detail in a forthcoming publication. The spectrum of Fig. 1 is taken under conditions where the $Y_D^{\bullet}$ contribution is minimized, but clearly some uncertainty exists on the exact lineshape and intensity of the $g \sim 2.00$ component.

The $S_1Y_Z^{\bullet}$ metalloradical EPR signal at W-band

Continuous-wave EPR spectra at W-band were obtained as described in the Materials and Methods section. The light minus dark difference signal obtained at 10 K is shown in Fig. 2 (Trace A). It is an average of 16 scans collected over a time period of *ca.* 20 min with the laser light on, minus the dark spectrum recorded approximately after 1 h dark adaptation at the same temperature. The difference spectrum is characterized by three main resonances at $g = 2.019$, 2.004 and 1.987. The signal at $g = 2.003$ is most probably a very small contribution from the carotenoid radical ($Car^{\bullet+}$), that was produced during the laser illumination and partially decayed during the one-hour dark-adaptation period that preceded the data collection for the dark spectrum. The assignment of this very narrow signal to $Car^{\bullet+}$ is based on its width and position, and a comparison with independent high-field (130 GHz[29] and 285 GHz[30]) EPR studies of this radical in Mn-depleted BBY membranes.

Theoretical simulation of the X- and W-band EPR spectra

In order to simulate the X- and W-band spectra (Traces A of Figs. 1 and 2 respectively), the spin-Hamiltonian in eqn. (1) was employed. In this Hamiltonian the assumption is made that the observed EPR signal is due to the magnetic interaction (*via* an exchange term) of two spins denoted S_a and S_b. S_a results from the S_1-state of the Mn-cluster and S_b from an organic radical attributed to $Y_Z^{\bullet}$ ($S_b = 1/2$).[23] No hyperfine terms are taken into account in this Hamiltonian. This is justified by the fact that the experimentally observed EPR signals are quite narrow with no evidence of any underlying broad signal. In addition, even though the direct assignment of the observed experimental peaks to specific energy transitions is not straightforward (*vide infra*), our simulations indicate that they are largely radical-based. The case considered here differs from the interaction between S_2 and $Y_Z^{\bullet}$ in inhibited PSII preparations.[8,9] The Mn cluster in the S_2 state is characterized by an isolated $S = 1/2$ ground state. The magnetic interactions therefore involve two $S = 1/2$ systems. Consequently the zero field splitting terms for the individual sites vanish and the number of the resulting levels is restricted to four. In the present case the Mn cluster in the S_1 state is an integer spin system for which the exact mapping of the spin manifolds is not known. In PSII particles from *Synechocystis* sp. PCC 6803 a multiline EPR signal at $g = 12$ deriving from the S_1-state has been detected in parallel mode.[31] A similar signal was also detected in spinach PSII membrane and core preparations depleted of the 23 and 17 kDa extrinsic proteins, but retaining the 33 kDa extrinsic protein.[32] In intact PSII membranes from spinach, the kind of preparations used in the present study, a broad structureless derivative-like EPR signal deriving from the S_1-state has been detected in parallel mode.[33,34] These studies[33,34] have suggested the existence of an $S_a = 0$ low-lying diamagnetic state with an $S_a = 1$ first excited state lying within thermal reach at liquid He temperatures. No other spin states have been detected or identified so far. In the present analysis we assume that the magnetic interaction between the radical and the Mn cluster in the S_1 state involves the two states $S_a = 0$ and $S_a = 1$.

The magnetic interaction between the radical and the cluster is expected to be weak ($<0.05\ cm^{-1}$), by analogy to the $S_2Y_Z^{\bullet}$ case in inhibited PSII preparations.[8,9] This is justified by the relatively large distance (>6 Å) between the centers, implied from the available structural information.[1–3] This weak exchange interaction is not expected to mix the $S_a = 0$ and $S_a = 1$ spin multiplets of the Mn cluster, which are separated by *ca.* 2–3 K (1.4–2.0 cm^{-1})[31,34] and it may thus be treated as a first order perturbation on the isolated S_a states. The magnetic interaction is expected also to be anisotropic because of dipolar interactions, which are not included explicitly in the present analysis. The effects of the anisotropy will be discussed later.

Zero field splitting terms (ZFS) lift the degeneracy of the $S_a = 1$ state. Earlier studies[31,34] have suggested that

$|D| = 0.12–0.14\ cm^{-1}$. These values were obtained from the S_1 state with reduced Y_Z. The oxidation of tyr Z in the present case may affect the ZFS values of the S_1-state *via* electrostatic interactions (*e.g.* proton exchange, see ref. 23).

The effect of the magnetic coupling is to afford two separate multiplets M1 and M2 (Scheme 1) associated with the $S_a = 0$ and $S_a = 1$ states of the Mn cluster, respectively. Multiplet M1 is characterized by a doublet whereas multiplet M2 gives rise to a sextet of states. At zero magnetic field the degeneracy of the sextet lifts due to the combined effect of the exchange interaction and the ZFS to afford three doublets (Scheme 1). Because ZFS and dipolar interactions have a similar mathematical formulation (both have the properties of a second rank tensor), they cannot be distinguished, and unavoidably these terms are strongly correlated in the analysis to be presented below. For simplicity we assume axial symmetry for both terms, and also that the principal axes systems coincide, allowing however for a 90° rotation. Accordingly E/D for the ZFS is set to 0 and two principal components of the $\boldsymbol{J}$ tensor are set equal.

Upon application of an external magnetic field the degeneracies of the various doublets are lifted. Mixing of the M1 and M2 multiplets can be neglected to a first approximation.[35] Fig. 3 shows the dependence of the energy levels of the two multiplets (M1, M2) on the external magnetic field, for an orientation parallel to the z-axis of the ZFS term. We observe that as the magnetic field increases a substate from the multiplet M2 decreases in energy much faster than the other substates. This substate is approximately the $|S_{az}, S_{bz}\rangle = |-1,-1/2\rangle$ of the system in the uncoupled representation. For a certain value of the magnetic field a level crossing between M1 and M2 takes place. The present experiments have been conducted at the two extreme ends of the diagram in Fig. 3, marked by arrows.

In the context of the above approximations EPR transitions at both frequency bands are confined within each of the multiplets M1 and M2 and no intermultiplet transitions are expected. The doublet from M1 is expected to behave essentially as the free radical (a signal II type spectrum), albeit with an enhanced relaxation rate. The spectra of the $S_1Y_Z^{\bullet}$ species produced by NIR excitation of the S_2 state[23] bear no or very little evidence for such a contribution. The X-band spectra produced by visible light excitation of S_1 contain, however, a signal II type component with a power saturation value ($P_{1/2}$) intermediate between the one of $Y_D^{\bullet}$ and the $g = 2.035$ signal (studies in progress). It is possible that the relative energy of the $S_a = 0$ and $S_a = 1$ spin manifolds is different in the two cases, with the $S_a = 0$ state being higher in energy (and therefore least populated) in the case of the production of the signal by NIR excitation of S_2. At the high power used in the present experiments the contribution from the $S_a = 0$ state (M1 multiplet) is saturated, and therefore its contribution to the spectrum of Fig. 1 minimized. Accordingly the main features of the spectra and particularly the components outside the $g = 2$ region are due to the magnetic interaction of the radical with the $S_a = 1$ spin state of the Mn cluster (M2 multiplet).

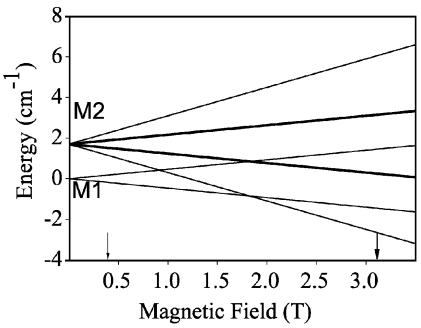

Fig. 3 Dependence of the energy levels on the external magnetic field applied parallel to the z-axis. Multiplets M1 and M2 are assumed to be separated by 1.7 cm^{-1} at zero magnetic field (see text). The arrows correspond approximately to the magnetic field regions where the signals are observed at X- (left arrow) and W-(left) band frequencies.

The g-values for $Y_Z^{\bullet}$ in Mn-depleted PSII were determined in a recent high field EPR study (245 GHz) by Un *et al.*[20] It was found that $g_x = 2.00750$, $g_y = 2.00422$ and $g_z = 2.00225$. A Gaussian width $\sigma_{g_x} = 0.0007$ was introduced to account for the distinctly broader feature for $Y_Z^{\bullet}$ at the g_x-edge relative to $Y_D^{\bullet}$, examined in the same publication. It was suggested that this broadening most probably reflects a distribution of magnetically and chemically distinct sites. These g-values for $Y_Z^{\bullet}$ in addition to σ_{g_x} were used as known fixed parameters in the calculation. Initial values of the parameters were determined by a simultaneous fit of both EPR spectra (X- and W-band) by allowing the values of the parameters $\boldsymbol{D}$, $\boldsymbol{J}$ and $\boldsymbol{g}$(metal center) to vary over reasonable limits. An early result of the analysis was that the three principal values of the exchange term, J_y and J_z were vanishingly small. These parameters were accordingly set to 0 and the subsequent analysis was based on the variation of J_x. In addition, a small distribution to the values of D, J_x and g_z-metal, denoted as σ_D, σ_J, σ_{gz} respectively had to be introduced for acceptable reproduction of the linewidths. Such distributions are not unusual and may be indicative of protein heterogeneity. They were taken as an indication of the error margin in the determination of the corresponding parameters.

The parameters extracted from the simultaneous fits of the X- and W-band EPR spectra (Traces B in Figs. 1 and 2 respectively) are quoted in Table 1. The theoretical spectra are compared with the experimental spectra in Figs. 1 and 2. Notably, all major features of the spectra are reproduced. As was noted above, the less accurate part of the experimental spectra is the $g = 2$ region. The simulations predict a $g = 2$ contribution accompanying the split components. The parameter that appears to affect the relative size of the $g = 2$ contribution in the theoretical calculations is the E/D. Future refinement of the experimental spectra in the $g = 2$ region will lead to more accurate estimation of this parameter, which is currently set to 0.

The tensor of the exchange interaction can be written in the form $\boldsymbol{J} = J_{iso}\boldsymbol{1} + \boldsymbol{D}_{ab}$ where $\boldsymbol{1}$ is the unitary tensor and $\boldsymbol{D}_{ab}$ is a traceless symmetric tensor.[36] From the data above we obtain $J_{iso} = -0.029(2)\ cm^{-1}$. The principal values of the $\boldsymbol{D}_{ab}$ tensor are $D_{ab} = -0.087\ cm^{-1}$ and $E_{ab}/D_{ab} = 0$. The tensors $\boldsymbol{D}_{ab}$ and $\boldsymbol{D}$ are found to have a common y-axis whereas the x- and z- axes are interchanged. As already discussed the ZFS term and the anisotropy of the exchange interactions cannot be determined independently. Thus the quoted numbers for these parameters must be viewed with caution and considered only as indicative.

$\boldsymbol{D}_{ab}$ mainly results from dipolar interactions. Due to its correlation with the ZFS term the value of this parameter cannot be unequivocally determined. We estimate, however, that the quoted value is an upper limit. Furthermore, because the two interacting spins are expected to be in close proximity (<10 Å) the point–dipole approximation is not applicable. One would need to have accurate information on the local electron spin density distribution on the four Mn-atoms of the cluster in the S_1-state and on the tyrosine radical, in order to safely account for the dipolar term.

Table 1 Simulation parameters of the spectra in Figs. 1 and 2[a]

Mn cluster in the S_1 state ($S_a = 1$)	D^b	−0.048 (2)[d]
	g_x	2.0055 (3)[d]
	g_y	2.0043 (2)[d]
	g_z	1.992 (3)[d]
Exchange interaction	$J_x{}^b$	−0.087 (2)[d]
	$J_y = J_z{}^b$	0.0[c]

[a] An axial ZFS tensor was employed ($E/D = 0$), [b] In cm^{-1}. [c] Fixed, [d] Numbers in parentheses are error estimates in the last digit.

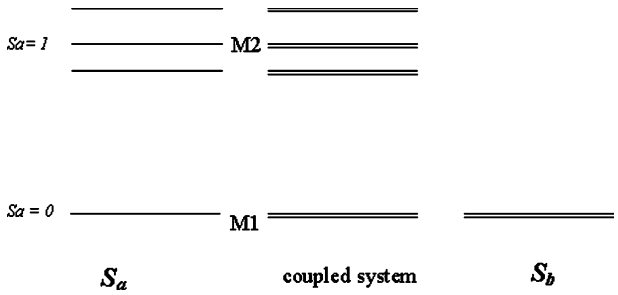

Scheme 1 The effect of the interaction between a spin coupled system with two low lying states (with $S_a = 0$ and $S_a = 1$) with an $S_b = 1/2$ system in the limit of weak exchange interaction at zero field. Double lines represent Kramers doublets.

The extracted exchange coupling is ferromagnetic ($J_{iso} < 0$). This is not unprecedented in the literature.[9,39–41] In PSII,[9] it has been shown that the $S_2Y_Z^{\bullet}$ signal in acetate-treated PSII membranes can be accurately simulated theoretically only by assuming a ferromagnetic exchange coupling between the Mn-cluster and the $Y_Z^{\bullet}$ radical.

At W band substates of the multiplet M2 lower in energy than the multiplet M1, (see Scheme 1), probably become the ground state. Further experiments are required to quantitate the contribution of these signals at high frequencies. It is very probable that under these conditions other states characterized by $S_a > 1$ may be operative.

In the literature many examples of weakly coupled spin systems can be found. In many cases, certain terms in Hamiltonian (1) (zero field splitting, exchange interactions or Zeeman terms) prevail over the others. This results in a rather small number of transitions rendering their assignment and interpretation quite straightforward.[37–41] In the present case the interactions involved are found to be of comparable magnitude. Under these conditions the number of expected transitions within the six levels is too large to allow for a direct assignment. To partially overcome this drawback we applied EPR spectroscopy at X- and W-bands. An inspection of the fits superimposed on the experimental spectra shows that, taking into account the large number of unknowns, the overall agreement is quite satisfactory. In order to check the validity of the derived parameters and better characterize the system by introducing more constraints, it is necessary to get additional data at other EPR frequencies, both higher and intermediate.

Acknowledgements

The authors wish to thank Dr Friedhelm Lendzian for helpful discussions and the hospitality during the conduction of the W-band experiments. This work was supported by DFG grant (Lu 315/16) on high-field EPR, by a TMR grant of the EU (No. FMRX-CT98-0214) and by Max Planck Society.

References

1 K. N. Fereira, T. M. Iverson, K. Maghlaoui, J. Barber and S. Iwata, *Science*, 2004, **303**, 1831–1838.
2 N. Kamiya and J. R. Shen, *Proc. Natl. Acad. Sci. USA*, 2003, **100**, 98–103.
3 A. Zouni, H. T. Witt, J. Kern, P. Fromme, N. Krauss, W. Saenger and P. Orth, *Nature*, 2001, **409**, 739–743.
4 P. Faller, C. Goussias, A. W. Rutherford and S. Un, *Proc. Natl. Acad. Sci. USA*, 2003, **100**, 8732–8735.
5 D. J. MacLachlan, J. H. Nugent, J. T. Warden and M. C. W. Evans, *Biochim. Biophys. Acta*, 1994, **1188**, 325–334.
6 J. M. Peloquin, K. A. Campbell and R. D. Britt, *J. Am. Chem. Soc.*, 1998, **120**, 6840–6841.
7 P. Dorlet, M. Di Valentin, G. T. Babcock and J. L. McCracken, *J. Phys. Chem. B*, 1998, **102**, 8239–8247.
8 K. V. Lakshmi, S. S. Eaton, G. R. Eaton, H. A. Frank and G. W. Brudvig, *J. Phys. Chem. B*, 1998, **102**, 8327–8335.
9 P. Dorlet, A. Boussac, A. W. Rutherford and S. Un, *J. Phys. Chem. B*, 1999, **103**, 10945–10954.
10 R. D. Britt, in *Advances in Photosynthesis: Vol. 4 Oxygenic Photosynthesis: The Light Reactions*, ed. R. D. Ort and C. F. Yocum, Kluwer Academic Publishers, Dordrecht, The Netherlands, 1996, pp. 137–164.
11 M. L. Gilchrist, J. A. Ball, D. W. Randall and R. D. Britt, *Proc. Natl. Acad. Sci. USA*, 1995, **92**, 9545–9549.
12 C. W. Hoganson, N. Lydakis-Simantiris, X.-S. Tang, C. Tommos, K. Warncke, G. T. Babcock, B. A. Diner, J. McCracken and S. Styring, *Photosynth. Res.*, 1995, **46**, 177–184.
13 C. W. Hoganson and G. T. Babcock, *Science*, 1997, **277**, 1953–1956.
14 M. Haumann, A. Mulkidjanian and W. Junge, *Biochemistry*, 1999, **38**, 1258–1267.
15 N. Ioannidis, J. H. A. Nugent and V. Petrouleas, *Biochemistry*, 2002, **41**, 9589–9600.
16 J. S. Vrettos, J. Limburg and G. W. Brudvig, *Biochim. Biophys. Acta–Bioenergetics*, 2001, **1503**, 229–245.
17 See refs. 10, 18 and 19 for recent reviews.
18 C. Goussias, A. Boussac and A. W. Rutherford, *Philos. Trans. R. Soc. London, Ser. B*, 2002, **357**, 1369–1381.
19 T. G. Carrell, A. M. Tyryskin and G. C. Dismukes, *J. Biol. Inorg. Chem.*, 2002, **7**, 2–22.
20 S. Un, X.-S. Tang and B. A. Diner, *Biochemistry*, 1996, **35**, 679–684.
21 W. Hofbauer, A. Zouni, R. Bittl, J. Kern, P. Orth, F. Lendzian, P. Fromme, H. T. Witt and W. Lubitz, *Proc. Natl. Acad. Sci. USA*, 2001, **98**, 6623–6628.
22 J. H. A. Nugent, I. P. Muhiuddin and M. C. W. Evans, *Biochemistry*, 2002, **41**, 4117–4126.
23 D. Koulougliotis, J.-R. Shen, N. Ioannidis and V. Petrouleas, *Biochemistry*, 2003, **42**, 3045–3053.
24 D. A. Berthold, G. T. Babcock and C. F. Yocum, *FEBS Lett.*, 1981, **134**, 231–234.
25 R. C. Ford and M. C. W. Evans, *FEBS Lett.*, 1983, **160**, 159–164.
26 C. Zhang and S. Styring, *Biochemistry*, 2003, **42**, 8066–8076.
27 A. Stesmans and G. van Gorp, *Rev. Sci. Instrum.*, 1989, **60**, 2949–2952.
28 A. P. Golombek and M. P. Hendrich, *J. Magn. Res.*, 2003, **165**, 33–48.
29 K. V. Lakshmi, M. J. Reifler, G. W. Brudvig, O. G. Poluektov, A. M. Wagner and M. C. Thurnauer, *J. Phys. Chem. B*, 2000, **104**, 10445–10448.
30 P. Faller, A. W. Rutherford and S. Un, *J. Phys. Chem. B*, 2000, **104**, 10960–10963.
31 K. A. Campbell, J. M. Peloquin, D. P. Pham, R. J. Debus and R. D. Britt, *J. Am. Chem. Soc.*, 1998, **120**, 447–448.
32 K. A. Campbell, W. Gregor, D. P. Pham, J. M. Peloquin, R. J. Debus and R. D. Britt, *Biochemistry*, 1998, **37**, 5039–5045.
33 S. L. Dexheimer and M. P. Klein, *J. Am. Chem. Soc.*, 1992, **114**, 2821–2826.
34 T. Yamauchi, H. Mino, T. Matsukawa, A. Kawamori and T. Ono, *Biochemistry*, 1997, **36**, 7520–7526.
35 We may assume for simplicity a dimer strongly coupled by antiferromagnetic exchange, comprising two spins $\boldsymbol{S}_A$, $\boldsymbol{S}_B$ with g-tensors $\boldsymbol{g}_A$ and $\boldsymbol{g}_B$. The Zeeman term may induce mixing between the multiplets of this exchange-coupled system through the term $Z_- = \beta \boldsymbol{B} \cdot \boldsymbol{g}_- \cdot \boldsymbol{V}$ where $\boldsymbol{g}_- = \boldsymbol{g}_A - \boldsymbol{g}_B$ and $\boldsymbol{V} = \boldsymbol{S}_A - \boldsymbol{S}_B$.[36] The Mn cluster in the S_1 state comprises Mn(III) and Mn(IV) ions for which the intrinsic g values are in the range 2.0–1.9. Hence $\boldsymbol{g}_-$ is small (<0.1) and the Z_- term may be neglected to a first approximation in the whole range of the magnetic fields used in this study.
36 A. Bencini and D. Gatteschi, in *EPR of Exchange Coupled Systems*, Springer-Verlag, Germany, 1990, pp. 57–85.
37 W. F. Butler, R. Calvo, D. R. Fredkin, R. A. Isaacson, M. Y. Okamura and G. Feher, *Biophys. J.*, 1984, **45**, 947–973.
38 A. Ivancich, P. Dorlet, D. B. Goodin and S. Un, *J. Am. Chem. Soc.*, 2001, **123**, 5050–5058.
39 A. L. P. Houseman, P. E. Doan, D. B. Goodin and B. M. Hoffman, *Biochemistry*, 1993, **32**, 4430–4443.
40 M. J. Benecky, J. E. Frew, N. Scowen, P. Jones and B. M. Hoffman, *Biochemistry*, 1993, **32**, 11929–11933.
41 W. R. Patterson, T. L. Poulos and D. B. Goodin, *Biochemistry*, 1995, **34**, 4342–4345.